Bacterial Ribonuclease MazF-Mediated Apoptosis as Potential Cancer Therapy

Maryam Saffarian Abbas Zadeh
Clemson University

Rebecca Anne MacPherson
Clemson University

Guohui Huang
Clemson University

Hui Ding
Clemson University

Rhonda Reigers Powell
Clemson University

Terri Bruce
Clemson University

Tzuen-Rong Jeremy Tzeng (✉ tzuenrt@clemson.edu)
Clemson University

---

1 Bacterial Ribonuclease MazF-Mediated Apoptosis as Potential Cancer Therapy

2 Maryam Saffarian Abbas Zadeh[1]; Rebecca Anne MacPherson[2]; Guohui Huang[1]; Hui Ding[1]; Rhonda

3 Reigers Powell[3]; Terri Bruce[3]; Tzuen-Rong Jeremy Tzeng*[1]

4

5 [1]Department of Biological Sciences, Clemson University, Clemson, SC, USA
6 [2]Department of Genetics and Biochemistry, Clemson University, Clemson, SC, USA
7 [3]Clemson Light Imaging Facility, Clemson University, Clemson, SC, USA
8

9 Corresponding author: Tzuen-Rong Jeremy Tzeng, tzuenrt@clemson.edu

10

Abstract:

Programmed cell death is a dynamic and critical mechanism of cell suicide in eukaryotes and prokaryotes. MazF is a ribonuclease protein involved in bacterial intracellular programmed death. This protein cleaves mRNAs at ACA sequences, leading to inhibition of protein synthesis and triggering cell death. Given that cancer is heterogenic and has varied susceptibility to treatment, we examined the impact of MazF proteins on the growth and viability of three cancer cell lines: MCF7, HT29, and AGS. These cell lines were transfected with ACA-less *mazF* mRNAs and evaluated for MazF-mediated cell death. The data illustrated that efficient MazF translation leads to a significant reduction in cell viability and is modulated by structural elements of ACA-less *mazF* mRNAs. In the presence of MazF, the levels of activated caspase-3 and -7 were significantly elevated in transfected cells, confirming the occurrence of apoptosis. We also quantified mRNA translation on a single-cell basis in MCF7 and AGS cell lines to examine MazF-mediated inhibition of protein synthesis. MazF expression significant decreases the levels of protein translation in the examined cell lines. This is the first report of MazF as a potential anti-cancer agent via induction of apoptosis in MCF7, AGS, and HT-29 cell lines.

Introduction:

Despite recent advances in treatment and diagnostic measures, cancer continues to plague the medical community and remains a major cause of mortality and morbidity worldwide [1]. Traditional cancer therapies also suffer from various limitations (e.g., the lack of specificity) and side effects including both temporary (e.g., diarrhea, nausea, loss of hair, and reduced resistance to infection) and long-term effects (e.g., decreased heart, lung, and kidney health). In an attempt to avoid some of these drawbacks, recent treatment efforts have focused on introducing certain drugs or small toxins with mild toxicities and tolerable immunogenicity [2].

1   As small proteins, ribonucleases have been a promising option in cancer therapy at the level of

2   gene expression [3] and function as anti-angiogenic, neurotoxic, antitumor, or immunosuppressive agents

3   against cancer [4,5]. These proteins occur naturally in both prokaryotic and eukaryotic cells. Bacteria

4   generate diverse groups of RNase proteins with various cytotoxic activities from anti-tumor effects to

5   involvement in bacterial programmed cell death (PCD) and population stability [6].

6   Bacteria are routinely exposed to harsh conditions, such as amino-acid starvation, antibiotics,

7   temperature change, and DNA damage, that lead to the regulation of cell growth and cell death [6]. Toxin-

8   antitoxin (TA) is an intracellular death mechanism present in almost all bacteria, comprising of bicistronic

9   operons containing a toxin and an antitoxin. In the TA system, toxins target processes such as DNA

10 replication, mRNA stability, protein synthesis, and ATP synthesis while their corresponding antitoxins

11 prevent toxin activities under normal conditions [7]. MazF is a well-studied toxin in bacteria that halts

12 protein translation but does not affect DNA or RNA synthesis. MazF protein targets specific sites in single-

13 stranded mRNAs, 16S rRNA, and transfer-messenger RNAs (tmRNAs), tRNA-mRNA hybrids that bind to the

14 aminoacyl site of ribosomes [6,8-10]. MazF degrades RNAs at either the 5′or the 3′ ends of the first A residue

15 of ACA sequences. Similar to RNase A, the 2-OH group at the cleavage site is crucial for the function of

16 MazF [11].

17   Shimazu et al. reported that MazF has the ability to impede protein synthesis and become

18 involved in Bak-dependent apoptosis in mammalian cells [12]. However, the injection of MazF DNA into solid

19 tumors, in spite of tumor shrinkages, did not prevent tumor regression. This failure stems from the

20 occurrence of mutations in the *mazF* gene, degradation of MazF or the lack of continued expression of

21 MazF in cells [13]. Therefore, DNA delivery may not be an optimal approach to deliver this RNase into cancer

22 cells or tumors.

23   *In vitro* transcribed mRNA (IVT mRNA)-based therapy, unlike other nucleic acid-based therapies,

24 offers exceptional advantages in the medical field. Translation in both dividing and non-dividing cells,

1 functionality in the cytoplasm, lack of immunogenic CpG motifs, expression independent of a strong

2 promoter or terminator, and no risk of genomic integration unlike viral and plasmid DNA have made

3 mRNA therapies valuable treatments against cancer [14,15]. The success of this therapy depends on many

4 factors, such as the quantity of *in vitro* transcription products, intracellular stability of IVT mRNA and its

5 translational efficiency, which can be influenced by caps, internal ribosome entry sites (IRES), poly-As,

6 Kozak sequences, codon composition and adjacent nucleotides [16]. In general, mRNA-based therapies, in

7 spite of their advantages, still face skepticism stemming from the instability and short half-life of mRNAs

8 [16].

9   In the present study, we evaluated the RNase activity of MazF in human MCF7 breast-, AGS

10 gastric-, and HT29 colorectal-adenocarcinoma cell lines for the first time. The influences of mRNA

11 structural elements, i.e., cap, IRES, poly-A tail, and Kozak sequence, on effective translation of transfected

12 mazF mRNA in these cell lines were also investigated.

13 Materials and Methods

14 *Plasmid Construction:*

15   pT7-*mazF* vector was generated by replacing GFP with ACA-less *mazF* in pcDNA3.3_eGFP

16 (Addgene, Watertown, MA, USA, cat. 26822) containing the T7 promoter. ACA-less *mazF* was amplified

17 from pBApo-*mazF* (kindly provided by Takara Bio Inc. Kusatsu, Japan) by using forward (5'-

18 ATGATAATATGGCCACAACCATGGTAAGCCGATACGT-3')   and   reverse   (5'-

19 GATAATTCTTAATTAATTCATCACCCAATCAGTACGTTAATTTTGGC-3') primers. pIRES-*mazF*-1 vector was

20 developed by substituting GFP with ACA-less *mazF* in pcDNA3.1(+) IRES (Addgene, cat. 51406) through

21 overlapping PCR. The ACA-less *mazF* fragment and the corresponding linear plasmids were ligated using

22 the NEB builder HIFI DNA (New England Biolabs, Ipswich, MA, USA, cat. E2621S) assembly kit according to

23 the manufacturer's instructions. Finally, the ligated products were electroporated into *Escherichia coli*

1   DH10B. Antisense *mazF* mRNA was synthesized against the 5' end of the *mazF* sequence. All designed

2   primers and antisense fragments were synthesized by Integrated DNA Technologies.

3   *mRNA Synthesis:*

4   T7-*mazF* and T7-GFP templates were amplified from pT7-*mazF* and pcDNA3.3_eGFP, respectively,

5   with forward (5'-TTGGACCCTCGTACAGAAGC TAATACG-3') and reverse (T120-CTTCCTA

6   CTCAGGCTTTATTCAAAGACCA) primers [17]. pcDNA3.1(+) IRES and pIRES-*mazF*-1 were used as the DNA

7   templates for T7-IRES-GFP and T7-IRES-*maz*F amplicons with forward (5'-AACCCACTGCTTA

8   CTGGCTTATCGAAATTAATACGAC-3') and reverse (5'-CCCTCTAGACTCGACTCTAGAAAGTGTCTCATGCCGG-

9   3') primers. The PCR products were used to generate mRNAs via a MEGAscript T7 kit (Thermo Fisher

10   Scientific, Waltham, MA, USA, cat. AM 1334). *In vitro* transcription (IVT) reactions were assembled with

11   ATP, CTP and GTP from a MEGAscript T7 kit, Pseudo-UTP (Ψ) (TriLink BioTechnologies, San Diego, CA, USA,

12   cat. N1019), Anti Reverse Cap Analog, 3′-O-Me-m^{7}G (5') ppp(5')G (TriLink BioTechnologies, cat. N-7003),

13   DNA templates, and T7 Polymerase (from MEGAscript T7 kit) and incubated at 37ºC overnight. To destroy

14   the DNA template and exclude the 5' triphosphates, the IVT reactions were first treated with Turbo DNase

15   (from MEGAscript T7 kit) and then Antarctic phosphatase (New England Biolabs, cat. M0289S). This was

16   followed by purification of IVT utilizing the RNeasy Mini Kit (Qiagen, Hilden, Germany, cat. 74104). The

17   quality of the RNA sample was analyzed by formaldehyde agarose gel electrophoreses. The mRNAs were

18   stored at -80 ºC.

19   *Cell Culture:*

20   HEK293, Human embryonic kidney 293 cells (ATCC®, Manassas, VA, USA, CR-1573) and MCF7

21   (ATCC® HTB-22) cells were maintained in Dulbecco's modified Eagle's medium (DMEM) with high glucose

22   and 2mM L-glutamine (ATCC® 30-2003). AGS (ATCC® CRL-1739) cells were grown in F12K medium (ATCC®

30-2004), while HT-29 (ATCC® HTB-38) cells were cultured in McCoys 5A medium (ATCC® 30-2007). All media were supplemented with 10% fetal bovine serum (Atlanta Biologicals, Inc., Flowery Branch, GA, USA . cat. S11095) and 1% penicillin/streptomycin (Thermo Fisher, cat. 15140122). Cells were maintained in fresh medium every 2 days at 37 ºC with 5% CO_2.

Transfection

All cell lines were seeded in concentrations of $5x10^5$ cells per well or $2.5x10^4$ cells per well in 6-well or 96-well plates, respectively. Transfection was carried out using Lipofectamine® MessengerMAX mRNA Transfection Reagent (Thermo Fisher, LMRNA003) following manufacturer's instructions.

Western Blot Analysis

Western blot assays were conducted using the anti-cleaved PARP monoclonal antibodies (Cell Signaling Technology, Danvers, MA, USA, cat. 9541S) and anti-actin monoclonal antibodies (Cell Signaling Technology, cat. 4970S). The transfected cells, in 6-well plates, were suspended in the lysing buffer (Cell Signaling Technology, cat. 9803S). The proteins present in the lysate were separated on a 10% SDS-PAGE gel and then transferred onto a PVDF membrane (Bio-Rad Laboratories, Hercules, CA, USA, cat. 1620174) via semi-dry electroblotting machine. The membranes were blocked (TBE, 5% dry milk powder, 0.1% Tween-20) for 1 hour at room temperature and incubated with antibodies overnight at 4 ºC. Horseradish peroxidase-conjugated secondary antibody (Cell Signaling Technology, cat. 7074S) and chemiluminescence substrate (Thermo Fisher, cat. 34580) were used to visualize actin and cleaved PARP.

Cell Viability Assay

The viability of transfected cells was analyzed via trypan blue exclusion. The cells were seeded in 6-well plates and transfected with *mazF* mRNA the following day. The transfected cells were trypsinized and counted using a hemocytometer.

6

The toxicity of *mazF* mRNA on different cell lines was determined using the MTT assay following the CellTiter 96® Non-Radioactive Cell Proliferation Assay (Promega, Madison, WI, USA cat. G4000) instructions.

Immunofluorescent Microscopy

The activation of caspase -3 and -7 was visualized under a fluorescence microscope (Motic AE31, Kowloon, Hong Kong) using an Image-iT LIVE Red caspase -3 and -7 Detection Kit (Thermo Fisher, cat. I35102).

Caspase Activity

Caspase -3 and -7 activity was measured using Caspase-Glo® 3/7 assay (Promega, cat. G8091) following the manufacturer's protocol.

Detection of Nascent Protein Synthesis

The transfected cells were prepared for analysis using the Click-iT Plus OPP Protein Synthesis Assay Kit (Thermo Fisher, C10458) following the manufacturer's instructions, with one modification: cells were fixed using 4% paraformaldehyde for 15 minutes instead of the recommended 3.7% formaldehyde. Following staining, samples were imaged using a GE IN Cell Analyzer 2500HS then analyzed using GE InCarta software (version 1.5). For analysis, we created a mask using HCS Nuclear Blue Stain.

Statistical Analysis

All experiments were conducted in triplicates. Data are shown as the mean ± standard deviation. The data were analyzed through t-tests. The difference was considered statistically significant when $P < 0.05$.

1   Results:

2   *mazF mRNA Structure*

3   mRNA therapy is an attractive approach for delivering genetic constructs into cells to treat a

4   disease. mRNA therapy owes its success to its superior transfection and expression efficiency, simplicity

5   and safety profile [18]. These advantages led us to examine whether ACA-less *mazF* mRNA can be effectively

6   transfected and translated in cancer cells. To this end, a T7–*mazF* construct (pT7-*mazF*) was designed. To

7   compare the expression efficacy of cap-dependent and IRES-dependent mRNAs for *in vitro* transcription

8   purposes, we developed a pIRES-*mazF*-1 plasmid. Additionally, several ACA-less *mazF* mRNAs lacking one

9   or more critical structural elements such as a cap, an IRES, poly-As, or Kozak sequences were constructed

10   and their effective translations in mammalian cells were measured.

11   Our results indicated that capped-*mazF*-polyadenylated or IRES-*mazF*-polyadenylated mRNA

12   could be translated in cells while the omission of any one of these mRNA structural elements, i.e., cap/IRES

13   or poly-As, was enough to block MazF protein expression. However, the lack of Kozak sequences did not

14   have any significant impacts on the expression of IRES-*mazF* mRNAs.

15   In mammalian cells, synthesized RNAs undergo nucleoside modifications that distinguish them

16   from exogenous RNA [14]. Kormann et al. suggested that the replacement of one of four basic nucleoside

17   triphosphates with a modified nucleotide blocks the interaction of mRNA with Toll-like receptors TLR3,

18   TLR7, TLR8 and retinoic acid-inducible gene I (RIG-I), which leads to the elimination of the immunogenicity

19   of exogenous mRNA [19]. In comparison to other modified nucleotides, the incorporation of pseudouridine

20   into synthesized mRNA has been reported to yield a higher level of mRNA translation and increase the

21   safety profile of such RNA therapies [18]. Therefore, *mazF* transcripts containing pseudouridine were also

22   evaluated for their translational ability in mammalian cells. In order to attribute MazF-mediated cell death

23   to the translation of transfected *mazF* mRNA, antisense *mazF* RNAs complementary to the 5' end of *mazF*

1 mRNA were co-transfected into AGS cells. Our results indicate that the partially double-stranded *mazF*

2 mRNA-antisense hybrid was sufficient to block effective translation of *mazF* mRNA resulting in reduced

3 cell death compared to cells transfected with *mazF* mRNA alone (Figure 1 i-j).

4 To examine the expression of *mazF* and GFP mRNAs in cancer cells, four versions of *mazF* and GFP

5 mRNAs were synthesized, i.e., capped and polyadenylated mRNA (C-mRNA-A), capped and

6 polyadenylated mRNA carrying pseudouridine (C-mRNA-psU-A), IRES and polyadenylated *mazF* mRNA

7 (IRES-mRNA-A), and IRES and polyadenylated mRNA with pseudouridine (IRES-mRNA-psU-A). The mRNAs

8 were then dephosphorylated with Antarctic phosphatase to prevent mRNAs from being recognized by

9 RIG-I, which is a sensor for viral RNAs [20]. HEK293, MCF7, AGS and HT29 cells were then transfected with

10 these *mazF* or GFP mRNAs. Monitoring transfected cells by fluorescence microscopy showed that cells

11 began to express GFP 6 hours after transfection. Cells exclusively translated C-GFP-A or mRNAs possessing

12 an IRES sequence and a poly-A tail (Figure 1 a-e). However, the fluorescence intensity of the IRES-GFP-A

13 was lower than that of capped GFP. IRES-GFP-A was expressed only in the AGS cell line (Figure 1d), while

14 the expression of IRES-GFP-A was not detectable in HT29, MCF7, and HEK293 cell lines.

15 Following the transfection, our results demonstrated that the expression of *mazF* mRNA in cells

16 arrested cell proliferation over the course of transfection. Significantly, HEK293 and AGS cells (Figure 1 f-

17 j) underwent extreme morphological changes 19 hours post transfection, while MCF7 and HT29 cells had

18 a severely reduced number of attached cells at 24 and 36 hours post transfection, respectively, suggesting

19 that MazF proteins were able to induce death in cancer cells.

20 The viability of MCF7, AGS, and HT29 cells expressing *mazF* mRNAs was determined using trypan

21 blue exclusion. As illustrated in Figure 2, when the cells were transfected with one of the four types of

22 mRNA mentioned above, the viability of cells was drastically reduced. An MTT-based cell viability assay

23 also indicated that the expression of MazF protein hampered cell metabolic activity and increased the

1   number of dead cells (data not shown). These data confirm that the expression of the MazF protein

2   induces death in the examined cancer cell lines.

3   *MazF-Mediated Apoptosis in Cancer Cells*

4   During stationary phase, MazF protein mediates cell death in *E. coli* by cleaving cellular mRNAs at

5   ACA sequences [10]. According to the findings of Shimazu et al., MazF protein has a similar ribonuclease

6   function in human HEK293 cell lines, i.e., the induction of apoptosis. To validate the induction of apoptosis

7   in different cancer cells, we examined whether activated Caspase-3 and -7 are present in transfected cells.

8   The Caspase-3 and -7 detection assay contains aspartic acid-glutamic acid-valine-aspartic acid (DEVD), a

9   caspase substrate that has a high affinity for activated caspases. Our results showed that the expression

10 of MazF caused apoptosis reactions in MCF7, AGS, and HT29 cells (Figure 3). MCF7, AGS, and HT29 cells

11 exhibited MazF-mediated apoptosis 12, 18, and 36 hours post transfection, respectively. Additionally, the

12 activity of caspase was quantified in these cell lines (Figure 3). Further, we investigated whether cleaved

13 PARP, a marker of cells undergoing apoptosis, was present in the cell lines translating mazF mRNA. As

14 shown in Figure 4, the cleaved PARP is detectable in AGS cells transfected with *mazF* mRNA. Altogether,

15 these results demonstrate that MazF could induce apoptosis in cancer cells.

16

17 *MazF-Mediated Inhibition of Protein Synthesis in Cancer Cells*

18   In *E. coli*, the activation of MazF protein leads to the inhibition of protein synthesis through

19 digestion of cellular mRNA [10]. Hence, we evaluated the inhibition of protein synthesis by MazF in MCF7,

20 AGS, and HT29 cell lines by quantifying mRNA translation on a single-cell basis. In this assay, an O-

21 propargyl-puromycin (OPP) is incorporated into *de novo* peptide chains and the generated chain is labeled

22 by photostable Alexa Fluor® dye. Fluorescence signals are then used to measure nascent protein

synthesis. As illustrated in Figure 5, MazF proteins significantly blocked synthesis of new proteins in the cells. Thus, our results confirm the translational interference role of MazF in the examined cell lines.

In *E. coli*, MazF cleaves mRNA at ACA sequences. GFP mRNA has 21 ACA sequences in the coding region. The co-transfection of C-*mazF*-A mRNAs with pcDNA3.3-egfp resulted in the decrease of GFP signal in transfected cells (Figure 6). This observation indirectly confirms that MazF is able to degrade mRNA and eventually block protein synthesis in transfected cells.

Discussion

Even with recent advancements in the medical field, cancer remains a significant concern. Introduction of novel therapies can bestow hope to many patients worldwide. Ribonucleases provide promising new treatment options that could be effective at transcription and translation levels. However, it quickly became evident that certain ribonucleases, due to their instability, the lack of cytotoxic or cytostatic activity, and the presence of ribonuclease inhibitors (RI) within cells making them poor candidates for cancer therapy [21].

MazF is a small and stable ribonuclease in bacterial cells that cleaves mRNAs, tRNA, and rRNA at ACA sequences. Under normal conditions, MazF binds a small, labile protein, i.e., MazE, and remains nontoxic in the cells. Under stressful conditions, MazE is degraded allowing MazF to arrest cell proliferation and induce death within bacterial cells [22]. The absence of a MazF inhibitor in mammalian cells encouraged us to investigate its potential application in cancer therapy. Shimazu et al. demonstrated that MazF is able to halt the growth of and induce apoptosis in T-REx-293 cells, a human kidney cell line. Given that cancer is a heterogeneous group of diseases with various sensitivities to different treatments, here we examined the impact of MazF on the growth and viability of three additional cancer cell lines, namely, MCF7, HT29 and AGS.

1   In this study, we demonstrated that the delivery of *mazF* mRNA into cancer cells enhances

2   translation of the encoded protein. mRNA is an attractive candidate in non-viral gene therapy due to its

3   ability to be active in the cytosol without entering the nucleus. However, mRNA lability has always

4   overshadowed the advantages of mRNA-based therapy. In order to address this concern, we studied the

5   necessity of the main structural elements of mRNA to boost the translation efficiency of MazF in *in vitro*

6   cell line conditions. Our results demonstrated that the presence of Cap/IRES and poly-A elements enables

7   the translation of the encoded protein within cells. We also synthesized and delivered GFP and *maz*F

8   mRNA into HEK293, MCF, AGS and HT29 cell lines. *mazF* mRNA deficient for caps or poly-As resulted in no

9   induction of death in transfected cells. These results may suggest synergy between cap structure and poly-

10   A tail in translation efficiency, a finding reported by various researchers [23-26]. This cooperation stems from

11   mRNA circulation, where the cap-eIF4E-eIF4G-PABP-poly-A complex hampers the function of

12   exonucleolytic nucleases in order to degrade mRNA [16].

13   The 5' ends of eukaryotic mRNAs contain a methylated m^7GpppN cap structure that is crucial for

14   mRNA splicing, stabilization, transport, and translation. In IVT reactions, the cap structure is linked to the

15   synthesized mRNA through an enzymatic reaction. However, this capping process caps either the 5' side

16   or both ends of the mRNA, rendering half of the synthesized mRNAs nonfunctional [16]. Recently, several

17   cap analogues have been designed to optimize the capping process in *in vitro* conditions. One example of

18   these cap analogs is the anti-reverse-cap analogue (ARCA), which contains a methylated 3'-OH group that

19   enforces ARCA to localize in the proper orientation [16].

20   Although the cap is a fundamental element in mRNA stability and translation, some viral and

21   cellular mRNAs possess internal ribosome entry sites (IRES) that carry out their translation in a cap-

22   independent manner. IRES sequences directly recruit ribosomes and start translation at either a non-AUG

23   codon or an overlapping +1 frame gene [27]. The discovery of IRES has led to an exciting path in cancer

24   therapy. This element enables researchers to design bicistronic, tricistronic or tetracistronic operons

1   encoding two or more genes under the control of a single promoter. Here, we recruited the IRES sequence

2   from encephalomyocarditis virus (EMCV) RNA to synthesize uncapped mRNAs. We then compared the

3   expression of capped and cap-independent mRNAs in cell-culture systems. As mentioned previously, both

4   IRES-*mazF*-A and C-*mazF*-A were expressed in the examined cell lines in a time-dependent manner.

5   However, each cell line differs in the expression of capped and IRES-dependent mRNAs and AGS cells are

6   more likely to express IRES-GFP-A than other cell lines. This indicates the probability that the type of mRNA

7   and cell line have significant influences on the expression of capped and cap-independent mRNAs. Our

8   results of transfected IVT mRNA in cells concur with that of other research groups [28-30]. Avci-Adali et al.

9   reported that, in spite of the high transfection efficacy, human endothelial cells and BJ human foreskin

10   fibroblasts express fewer copies of capped GFP proteins in comparison to HEK293 [29].

11   Another problem that overshadows the advantages of the IVT mRNA technique is mRNA

12   immunogenicity. Several investigations have indicated that certain innate immune receptors such as TLR3,

13   TLR7, TLR8 and RIG-I may be stimulated by exogenous RNA [17]. The incorporation of modified nucleosides,

14   e.g., pseudouridine or 2-thiouridine (s^2U) in IVT mRNA, and the elimination of 5' triphosphates from

15   synthesized mRNA can suppress the activation of TLRs and RIG-I [29,31]. Previous research showed that

16   inclusion of pseudouridine in mRNA structures significantly enhances the translation efficiency of the

17   encoded proteins when compared to mRNAs possessing unmodified uridines [29,32,33]. This difference stems

18   from the diminished activity of protein kinase ribonuclease (PKR) in the presence of mRNAs that contain

19   modified nucleotides [31]. It seems that pseudouridine has the ability to enhance stability and boost the

20   expression of IVT mRNAs in comparison to other modified nucleotides [33]. Our results, however, varied

21   slightly from those of previous studies. Our data showed that the presence of modified nucleotides in the

22   structure of IRES-GFP did not lead to an increased expression of encoded proteins in cells. Our data also

23   highlighted the role of each cell line on the expression of IVT mRNAs containing either modified or non-

24   modified nucleotides.

1 As a part of their defense responses, eukaryotic and prokaryotic cells have the capability to

2 degrade mRNA and subsequently suppress protein synthesis. For example, when bacteria are exposed to

3 harsh conditions (e.g., extreme amino acid starvation or antibiotic-blocked transcription or translation),

4 they use MazF proteins to cleave mRNAs and therefore block protein synthesis [34,35]. In mammalian cells,

5 some of the host antiviral responses that lead to inhibition of protein synthesis and eventually to induction

6 of apoptosis in virus-infected cells including the interferon response, RNaseL-mediated degradation of

7 28S and 18S ribosomal RNAs, and the activation of protein kinase-R [36]. However, the dependency of cancer

8 on protein synthesis can be targeted by inhibition of nascent protein synthesis ribonuclease-based

9 therapy [37]. We analyzed the impact of MazF proteins on the inhibition of protein synthesis, which resulted

10 in the induction of apoptosis in MCF7, AGS and HT29 cell lines. In this study, nascent protein synthesis

11 was determined through measuring the incorporation of O-propargyl-puromycin (OPP) into newly

12 synthesized proteins. Our observations confirmed that the overexpression of MazF leads to a drastic drop

13 in the levels of protein translation in the examined cell lines. These results are consistent with the study

14 conducted by Shimazu et al. which demonstrated that the level of protein synthesis was reduced in T-REx-

15 293 cells 24 hours post transfection with MazF mRNA. In addition, our results suggested that the reduction

16 of protein synthesis mediated by MazF was cell line dependent.

17 In mammals, the inhibition of protein synthesis leads to apoptosis and cell death, although the

18 exact mechanisms remain unknown [38]. Here, our data illustrated that MazF not only stopped the

19 proliferation of cells but also significantly reduced the number of living cells 18 to 24 hours post

20 transfection in tested cell lines. In order to confirm the occurrence of apoptosis, the activation of caspase-

21 3 and -7 and the presence of caspase 3's substrate was evaluated in transfected cells. Our observations

22 suggested that in the presence of MazF, the level of caspase-3 and -7 significantly increased and apoptosis

23 occurred in the cells. These data confirm the antiproliferative action and apoptotic ability of MazF in

24 cancer cells. Interestingly, MazF was able to induce apoptosis in MCF7 cells that are supposedly apoptosis-

1 resistant. These cells are deficient for caspase-3 and also are resistant to ionizing radiation (IR)-induced

2 apoptosis [39]. Essman et al. demonstrated that the exposure of MC7 to methylxanthine caffeine and the

3 staurosporine analogue UCN-01 did not lead to the activation of the initiator caspase-9 and the cells

4 remained resistant to apoptosis [39]. Therefore, according to our results, MazF may serve as a suitable

5 therapeutic candidate against MCF7. As we have demonstrated, MazF successfully induced death in AGS

6 and HT29 cell lines. These cell lines have been reported to possess long non-coding RNA GACAT1

7 (lncGACAT1) and long non-coding RNA (lncRNA) Gas5, respectively, that stimulate cell proliferation and

8 invasion [40,41]. These non-coding RNAs contain several ACA sites in their sequences that potentially make

9 the non-coding RNAs more vulnerable to the action of MazF.

10 In conclusion, we described the use of MazF, a bacterial ribonuclease, for induction of apoptosis

11 in three different cell lines. We also investigated the influence of IRES, a cap structure, and the

12 incorporation of modified nucleotides on the expression of the encoded protein. Our results showed that

13 although cell lines have a varying preference for translation of the delivered mRNAs, the delivered *mazF*

14 mRNA was expressed and the MazF protein was able to inhibit *de novo* protein translation. Thus, it seems

15 MazF has great potential to serve as a therapeutic agent for cancer treatment.

16 Additional Information

17 *Acknowledgements*

20 *Competing Interests Statement*

21 The authors declare that they have no competing financial and non-financial interests.

1 *Funding*

9

10

References

1   Beebe, S. J., Sain, N. M. & Ren, W. Induction of Cell Death Mechanisms and Apoptosis by Nanosecond Pulsed Electric Fields (nsPEFs). *Cells* **2**, 136-162, doi:10.3390/cells2010136 (2013).

2   Makarov, A. A. & Ilinskaya, O. N. Cytotoxic ribonucleases: molecular weapons and their targets. *FEBS Letters* **540**, 15-20, doi:https://doi.org/10.1016/S0014-5793(03)00225-4 (2003).

3   Fang, E. F. & Ng, T. B. Ribonucleases of different origins with a wide spectrum of medicinal applications. *Biochimica et Biophysica Acta (BBA) - Reviews on Cancer* **1815**, 65-74, doi:https://doi.org/10.1016/j.bbcan.2010.09.001 (2011).

4   Schein, C. H. From housekeeper to microsurgeon: the diagnostic and therapeutic potential of ribonucleases. *Nature biotechnology* **15**, 529-536, doi:10.1038/nbt0697-529 (1997).

5   D'Alessio, G. New and cryptic biological messages from RNases. *Trends in cell biology* **3**, 106-109 (1993).

6   Engelberg-Kulka, H., Amitai, S., Kolodkin-Gal, I. & Hazan, R. Bacterial programmed cell death and multicellular behavior in bacteria. *PLoS Genet* **2** (2006).

7   Yamaguchi, Y., Park, J. H. & Inouye, M. Toxin-antitoxin systems in bacteria and archaea. *Annu Rev Genet* **45**, 61-79 (2011).

8   Engelberg-Kulka, H., Hazan, R. & Amitai, S. mazEF: a chromosomal toxin-antitoxin module that triggers programmed cell death in bacteria. *J Cell Sci* **118**, 4327-4332 (2005).

9   Bertram, R. & Schuster, C. F. Post-transcriptional regulation of gene expression in bacterial pathogens by toxin-antitoxin systems. *Front Cell Infect Microbiol* **4** (2014).

10   Zhang, Y. *et al.* MazF cleaves cellular mRNAs specifically at ACA to block protein synthesis in Escherichia coli. *Molecular cell* **12**, 913-923 (2003).

11   Zhang, Y., Zhang, J., Hara, H., Kato, I. & Inouye, M. Insights into the mRNA cleavage mechanism by MazF, an mRNA interferase. *J Biol Chem* **280**, 3143-3150 (2005).

12   Shimazu, T. *et al. NBK/BIK antagonizes MCL-1 and BCL-X(L) and activates BAK-mediated apoptosis in response to protein synthesis inhibition.* (Genes Dev. 2007 Apr 15;21(8):929-41. doi:10.1101/gad.1522007.).

13   Shimazu, T., Mirochnitchenko, O., Phadtare, S. & Inouye, M. Regression of Solid Tumors by Induction of MazF, a Bacterial mRNA Endoribonuclease *J Mol Microbiol Biotechnol* **24**, 228–233, doi:10.1159/000365509 (2014).

14   Sahin, U., Kariko, K. & Tureci, O. mRNA-based therapeutics [mdash] developing a new class of drugs. *Nat Rev Drug Discov* **13**, 759-780, doi:10.1038/nrd4278 (2014).

15   Sergeeva, O. V., Koteliansky, V. E. & Zatsepin, T. S. mRNA-Based Therapeutics - Advances and Perspectives. *Biochemistry. Biokhimiia* **81**, 709-722, doi:10.1134/s0006297916070075 (2016).

16   Tavernier, G. *et al.* mRNA as gene therapeutic: how to control protein expression. *Journal of controlled release : official journal of the Controlled Release Society* **150**, 238-247, doi:10.1016/j.jconrel.2010.10.020 (2011).

17   Avci-Adali, M. *et al.* Optimized conditions for successful transfection of human endothelial cells with in vitro synthesized and modified mRNA for induction of protein expression. *Journal of Biological Engineering* **8**, 8, doi:10.1186/1754-1611-8-8 (2014).

18   Kariko, K. *et al.* Incorporation of pseudouridine into mRNA yields superior nonimmunogenic vector with increased translational capacity and biological stability. *Molecular therapy : the journal of the American Society of Gene Therapy* **16**, 1833-1840, doi:10.1038/mt.2008.200 (2008).

19   Kormann, M. S. *et al.* Expression of therapeutic proteins after delivery of chemically modified mRNA in mice. *Nature biotechnology* **29**, doi:10.1038/nbt.1733 (2011).

20   Kell, A. M. & Gale, M., Jr. RIG-I in RNA virus recognition. *Virology* **479-480**, 110-121, doi:10.1016/j.virol.2015.02.017 (2015).

21   Ardelt, W., Ardelt, B. & Darzynkiewicz, Z. Ribonucleases as potential modalities in anticancer therapy. *European journal of pharmacology* **625**, 181-189, doi:10.1016/j.ejphar.2009.06.067 (2009).

22   Wang, N. R. & Hergenrother, P. J. A Continuous Fluorometric Assay for the Assessment of MazF Ribonuclease Activity. *Analytical biochemistry* **371**, 173-183, doi:10.1016/j.ab.2007.07.017 (2007).

23   Preiss, T., Muckenthaler, M. & Hentze, M. W. Poly(A)-tail-promoted translation in yeast: implications for translational control. *RNA* **4**, 1321-1331 (1998).

24   Gallie, D. R. The cap and poly(A) tail function synergistically to regulate mRNA translational efficiency. *Genes & Dev* **5**, 2108-2116, doi:10.1101/gad.5.11.2108 (1991).

25   Mockey, M. *et al.* mRNA transfection of dendritic cells: Synergistic effect of ARCA mRNA capping with Poly(A) chains in cis and in trans for a high protein expression level. *Biochemical and Biophysical Research Communications* **340**, 1062-1068, doi:https://doi.org/10.1016/j.bbrc.2005.12.105 (2006).

26   Michel, Y. M., Poncet., D., Piron, M., Kean, K. M. & Borman, A. W. Cap-Poly(A) synergy in mammalian cell-free extracts. Investigation of the requirements for poly(A)-mediated stimulation of translation initiation. *The Journal of Biological Chemistry* **275**, 32268-32276, doi:doi: 10.1074/jbc.M004304200 (2000).

27   Wang, Q. S. & Jan, E. Switch from Cap- to Factorless IRES-Dependent 0 and +1 Frame Translation during Cellular Stress and Dicistrovirus Infection. *PLoS ONE* **9**, e103601, doi:10.1371/journal.pone.0103601 (2014).

28   Xi, S. *et al.* IRES-Mediated Protein Translation Overcomes Suppression by the p14ARF Tumor Suppressor Protein. *Journal of Cancer* **8**, 1082-1088, doi:10.7150/jca.17457 (2017).

29   Avci-Adali, M. *et al.* Optimized conditions for successful transfection of human endothelial cells with in vitro synthesized and modified mRNA for induction of protein expression. *J Biol Eng* **8**, 8, doi:10.1186/1754-1611-8-8 (2014).

30   Avci-Adali, M. *et al.* In Vitro Synthesis of Modified mRNA for Induction of Protein Expression in Human Cells. *Journal of Visualized Experiments : JoVE*, 51943, doi:10.3791/51943 (2014).

31   Anderson, B. R. *et al.* Incorporation of pseudouridine into mRNA enhances translation by diminishing PKR activation. *Nucleic Acids Research* **38**, 5884-5892, doi:10.1093/nar/gkq347 (2010).

32 Hornung, V. *et al.* 5'-Triphosphate RNA is the ligand for RIG-I. *Science (New York, N.Y.)* **314**, 994-997, doi:10.1126/science.1132505 (2006).

33 Karikó, K., Buckstein, M., Ni, H. & Weissman, D. Suppression of RNA Recognition by Toll-like Receptors: The Impact of Nucleoside Modification and the Evolutionary Origin of RNA. *Immunity* **23**, 165-175, doi:10.1016/j.immuni.2005.06.008 (2005).

34 Zhang, Y. *et al.* MazF cleaves cellular mRNAs specifically at ACA to block protein synthesis in Escherichia coli. *Mol Cell* **12**, 913-923 (2003).

35 Gerdes, K. & Maisonneuve, E. Bacterial persistence and toxin-antitoxin loci. *Annu Rev Microbiol* **66**, 103-123 (2012).

36 Gil, J. & Esteban, M. Induction of apoptosis by the dsRNA-dependent protein kinase (PKR): mechanism of action. *Apoptosis : an international journal on programmed cell death* **5**, 107-114 (2000).

37 Martineau, Y., Müller, D. & Pyronnet, S. Targeting protein synthesis in cancer cells. *Oncoscience* **1**, 484-485 (2014).

38 Shimazu, T. *et al.* NBK/BIK antagonizes MCL-1 and BCL-X(L) and activates BAK-mediated apoptosis in response to protein synthesis inhibition. *Genes & Development* **21**, 929-941, doi:10.1101/gad.1522007 (2007).

39 Essmann, F., Engels, I. H., Totzke, G., Schulze-Osthoff, K. & Jänicke, R. U. Apoptosis Resistance of MCF-7 Breast Carcinoma Cells to Ionizing Radiation Is Independent of p53 and Cell Cycle Control but Caused by the Lack of Caspase-3 and a Caffeine-Inhibitable Event. *Cancer Research* **64**, 7065-7072, doi:10.1158/0008-5472.can-04-1082 (2004).

40 Wang, D., Ji, Y., Li, W., Yu, Y. & Liu, C. Long non-coding RNA GACAT1promotes proliferation and invasion of gastric cancercells by targeting miR-378. *Int J Clin Exp Pathol* **10**, 6364-6374 (2017).

41 Li, J. *et al.* Effect of long non-coding RNA Gas5 on proliferation, migration, invasion and apoptosis of colorectal cancer HT-29 cell line. *cancer cell int.* **18**, doi:10.1186/s12935-018-0510-6 (2018).

1 **Author Contributions Statement**

2 Saffarian Abbas Zadeh and Tzeng defined the scope of work, designed the experiments, analyzed the

3 results and prepared the manuscript; Saffarian Abbas Zadeh constructed all the vectors used in this study;

4 Saffarian Abbas Zadeh, MacPherson, Huang, and Ding carried out the designed bioassays; Powell and

5 Bruce measured and analyzed the impact of MazF on the levels of nascent protein synthesis reported in

6 Figure 5. All authors read and approved the final manuscript.

7 **Figure Legends**

8 Figure 1: The translation of GFP and *mazF* mRNAs in cancer cells 24 hours post transfection. a) and c), cells

9 were transfected with C-GFP-A mRNAs; d) AGS was transfected with IRES-GFP-A; b), e), f) are non-

10 transfected AGS cells; g) AGS cells were transfected by GFP mRNA; h), AGS cells were transfected by *mazF*

11 mRNA; i) AGS cells were co-transfected by *mazF* mRNA and antisense mRNAs; j) AGS cells were transfected

12 by antisense mRNA and served as the control. a-e are fluorescence images and f-j are bright-field images.

13

14

15 Figure 2: The expression of MazF results in a significant reduction in cell viability in transfected a) AGS and

16 b) MCF7 cell lines. (n=3)

17

18

19 Figure 3: MazF-mediated apoptosis in transfected MCF7 (a1-3) and HT29 (b1-3) cell lines; a1 and b1: The

20 expression of MazF leads to caspase activity in transfected cells; a2-3, b2-3: Fluorescent cells under the

21 fluorescence microscope indicating the activation of caspase in transfected cells. (n=3)

22

23

24 Figure 4: The presence of cleaved-PARP in lysates of transformed AGS cells 18 hours post induction of

25 MazF visualized via Western blot. β-actin was used as the loading control and blotted separately. Images

26 for β-actin and cleaved-PARP gels were cropped and aligned. The original exposures and contrast levels

27 were maintained. The original Western blot raw data and construction of the figure are in the

28 Supplementary information file. Ladder: Precision Plus protein™ (BioRAD, cat. 1610373).

29

30

1   Figure 5: Impaired protein translation in a1) MCF7 and b1) AGS mediated by MazF. a2, b2: The reduction

2   of fluorescence (red signals) indicated the inhibition of nascent protein synthesis in transfected cells. The

3   nucleases were stained with NuclearMask Blue stain, (n=3).

4

5

6   Figure 6: Impact on pcDNA3.3-egfp expression in C-*mazF*-A mRNA transfected HEK 293 cells. a) Abundant

7   GFP expression in HEK293; b) Reduced GFP expression in C-*mazF*-A mRNA transfected HEK 293 cells.

Figures
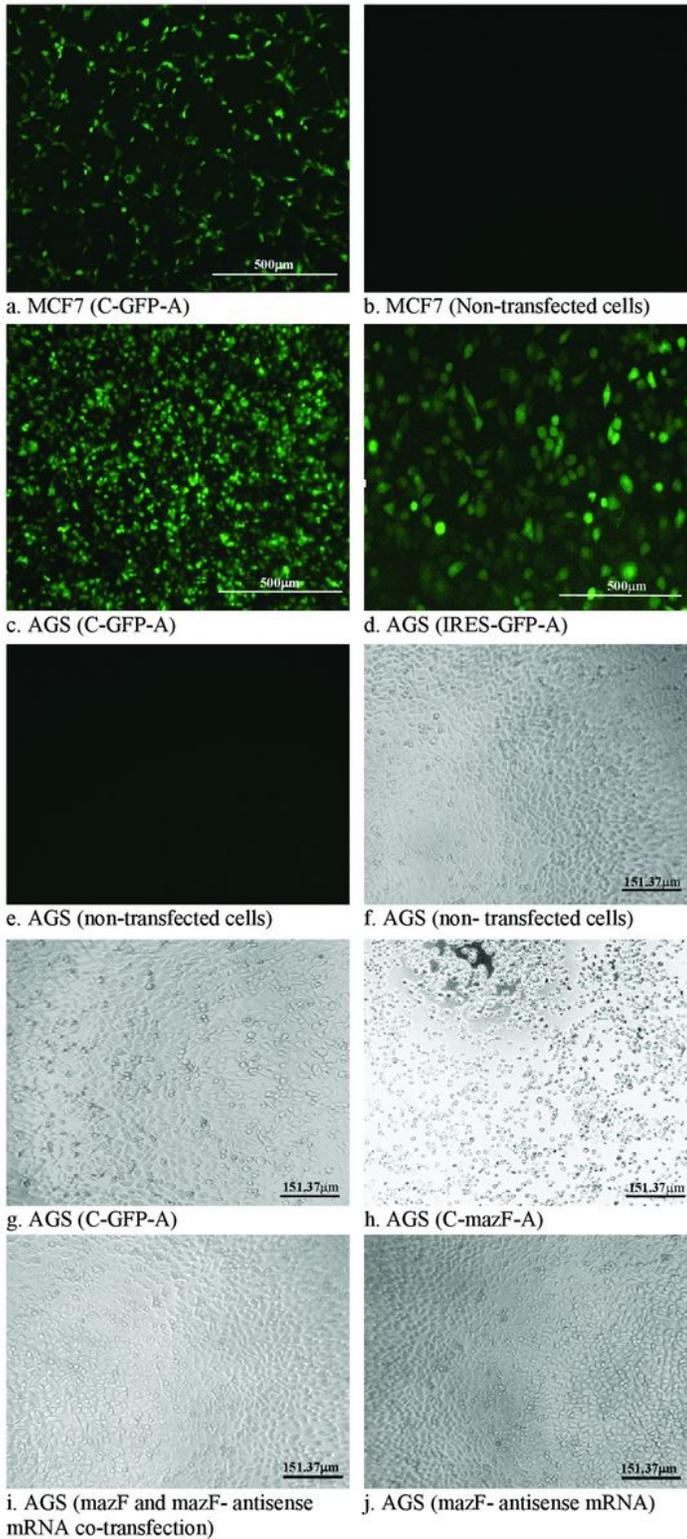
a. MCF7 (C-GFP-A)

b. MCF7 (Non-transfected cells)

c. AGS (C-GFP-A)

d. AGS (IRES-GFP-A)

e. AGS (non-transfected cells)

f. AGS (non- transfected cells)

g. AGS (C-GFP-A)

h. AGS (C-mazF-A)

i. AGS (mazF and mazF- antisense mRNA co-transfection)

j. AGS (mazF- antisense mRNA)

Figure 1

The translation of GFP and mazF mRNAs in cancer cells 24 hours post transfection. a) and c), cells were transfected with C-GFP-A mRNAs; d) AGS was transfected with IRES-GFP-A; b), e), f) are non-transfected AGS cells; g) AGS cells were transfected by GFP mRNA; h), AGS cells were transfected by mazF mRNA; i)

AGS cells were co-transfected by mazF mRNA and antisense mRNAs; j) AGS cells were transfected by antisense mRNA and served as the control. a-e are fluorescence images and f-j are bright-field images.
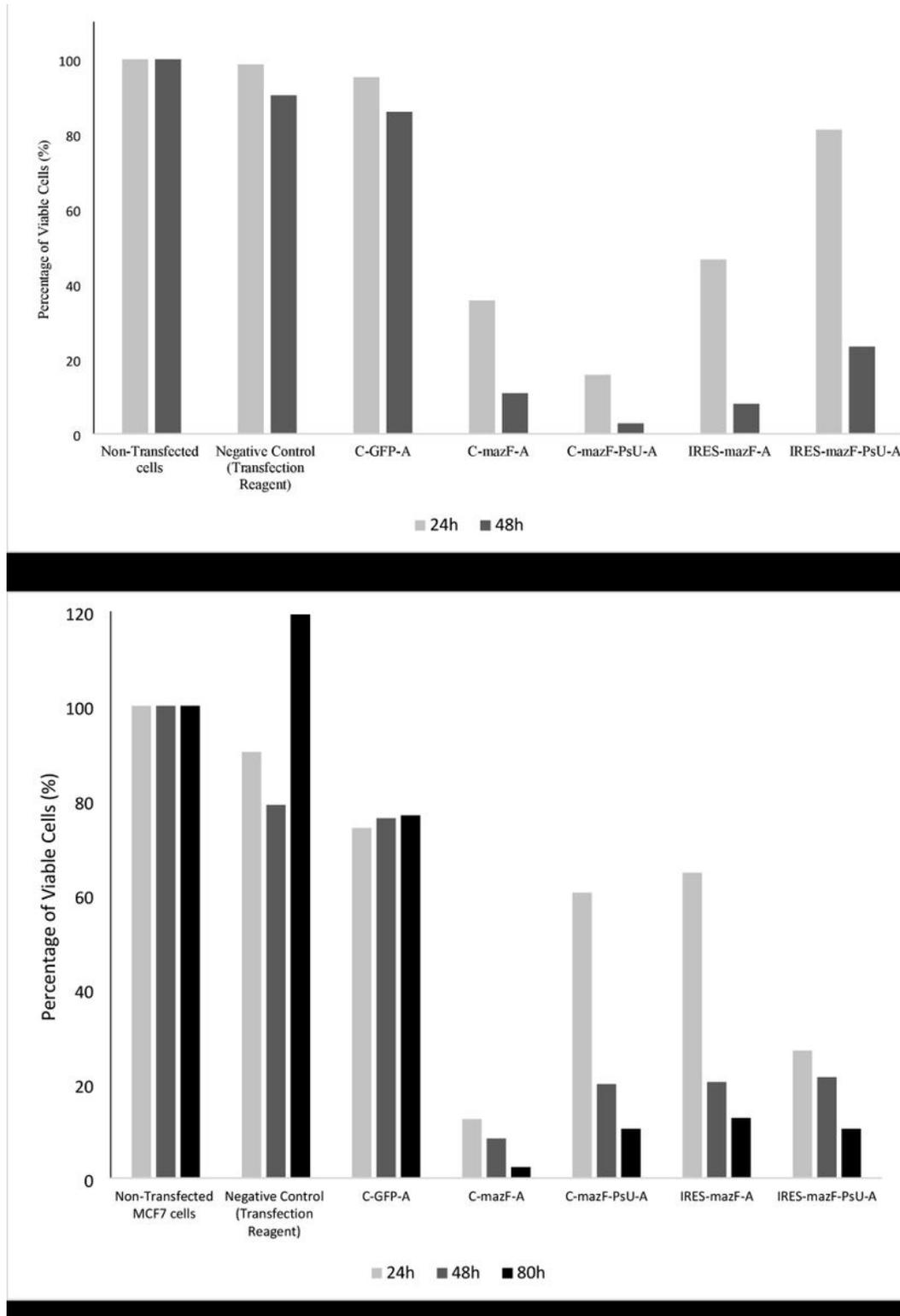
Figure 2

The expression of MazF results in a significant reduction in cell viability in transfected a) AGS and b) MCF7 cell lines. (n=3)

a₁. MCF7 cells

a₂. MCF7 cells transfected with C-*mazF*-A

a₃. Non-transfected MCF7 cells

b₁. HT29 cells

b₂. HT29 cells transfected with C-*mazF*-A
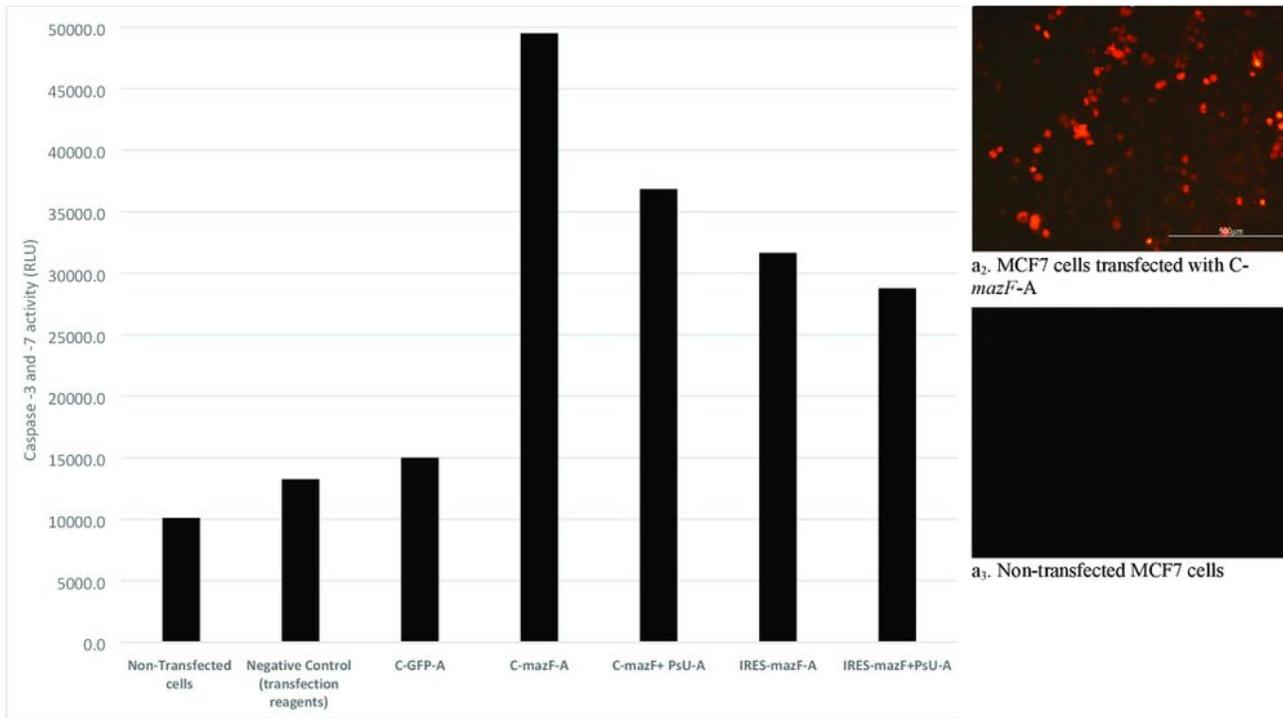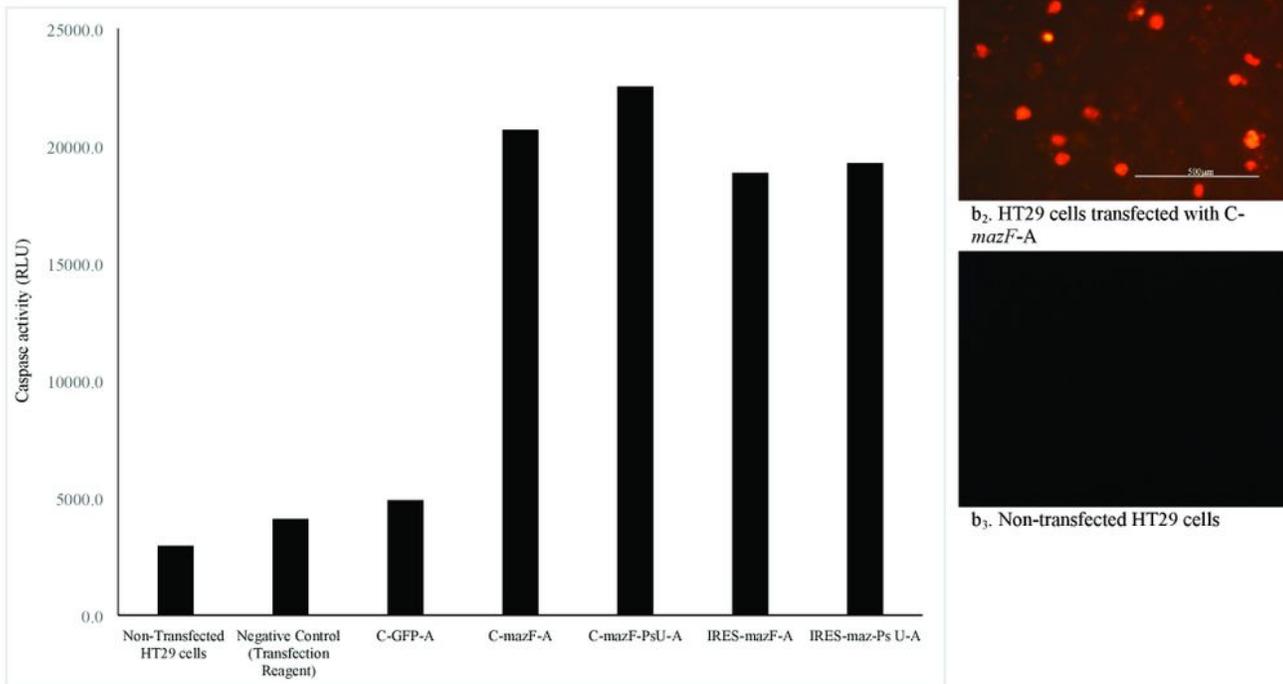
b₃. Non-transfected HT29 cells

Figure 3

MazF-mediated apoptosis in transfected MCF7 (a1-3) and HT29 (b1-3) cell lines; a1 and b1: The expression of MazF leads to caspase activity in transfected cells; a2-3, b2-3: Fluorescent cells under the fluorescence microscope indicating the activation of caspase in transfected cells. (n=3)
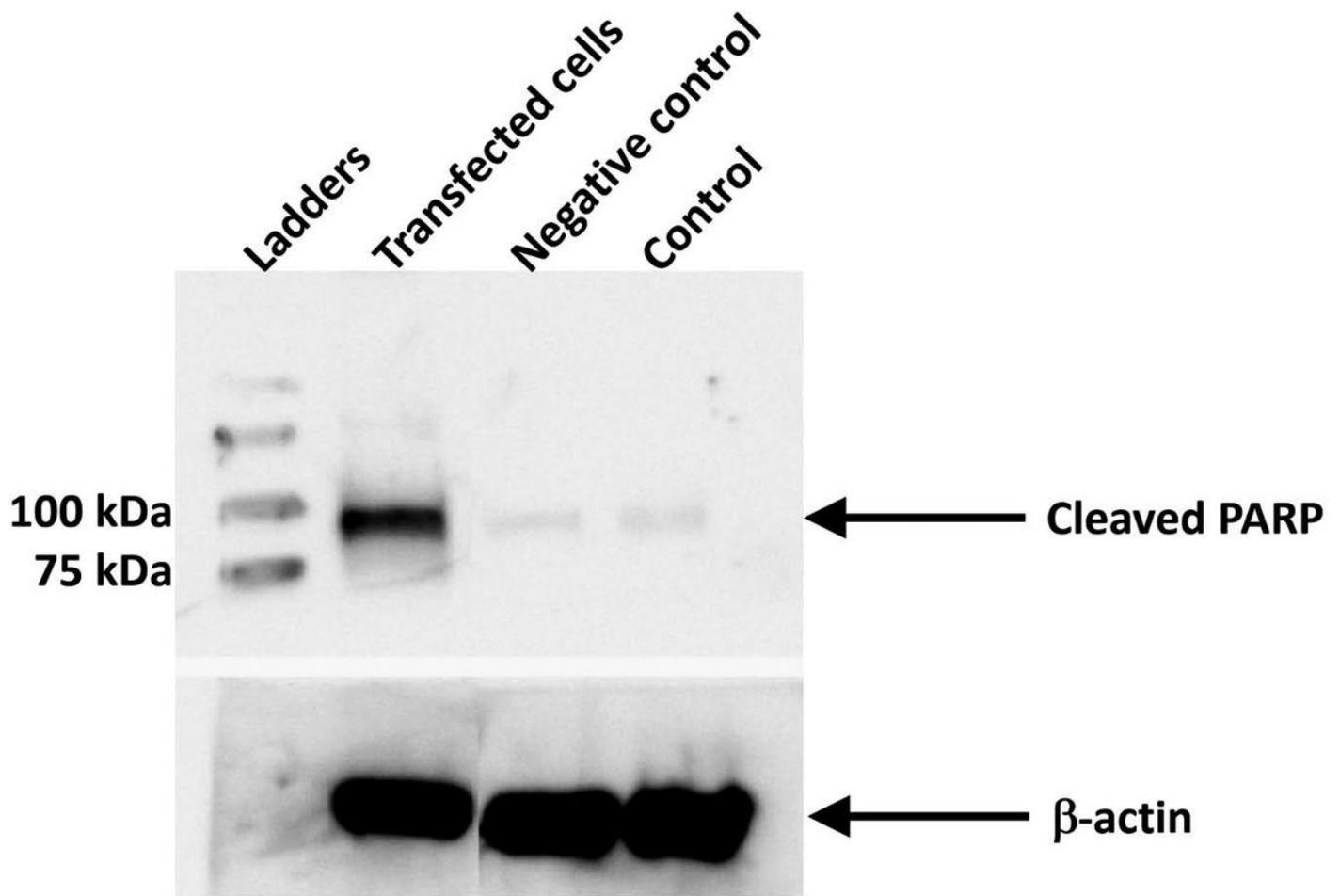
Figure 4

The presence of cleaved-PARP in lysates of transformed AGS cells 18 hours post induction of MazF visualized via Western blot. β-actin was used as the loading control and blotted separately. Images for β-actin and cleaved-PARP gels were cropped and aligned. The original exposures and contrast levels were maintained. The original Western blot raw data and construction of the figure are in the Supplementary information file. Ladder: Precision Plus protein™ (BioRAD, cat. 1610373).
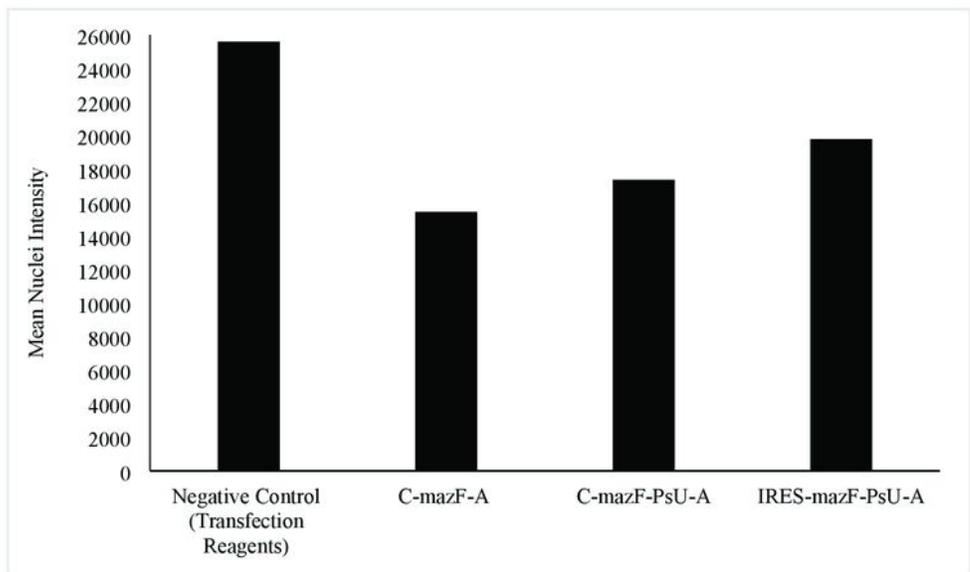
a$_1$. MCF7
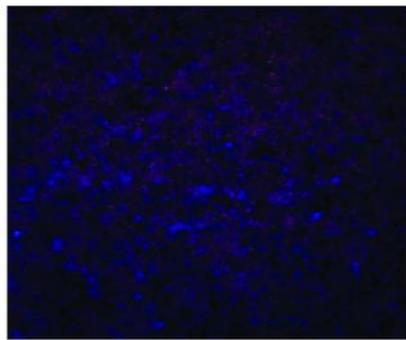
a$_2$. MCF7 cells transfected with C-mazF-A
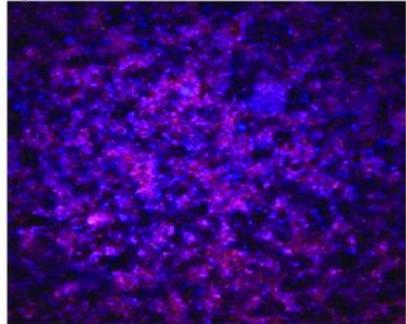
a$_3$. Control cells (MCF7)
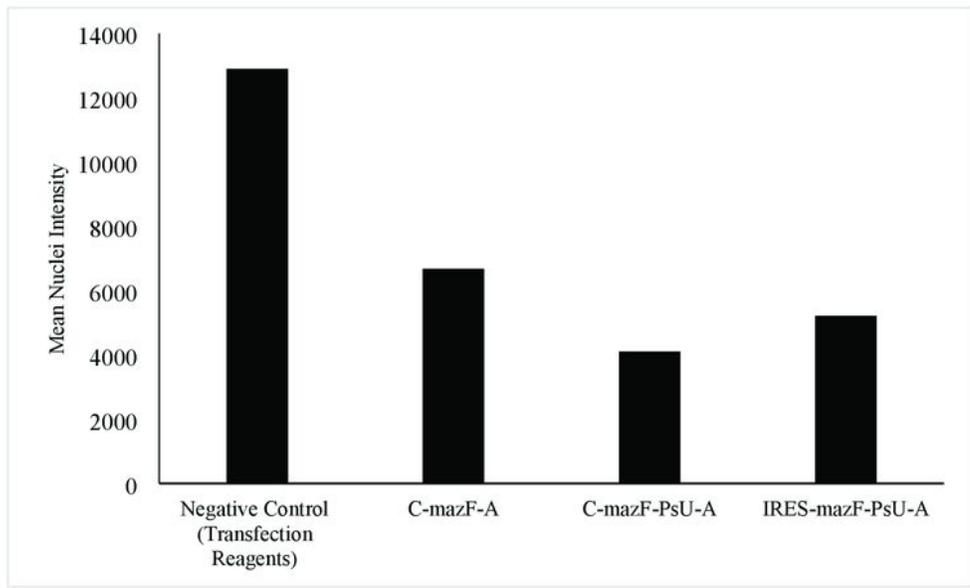
b$_1$. AGS
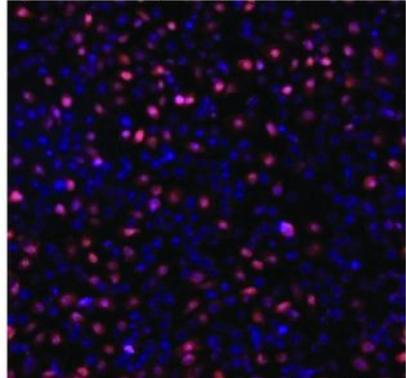
b$_2$. AGS cells transfected with C-mazF-A
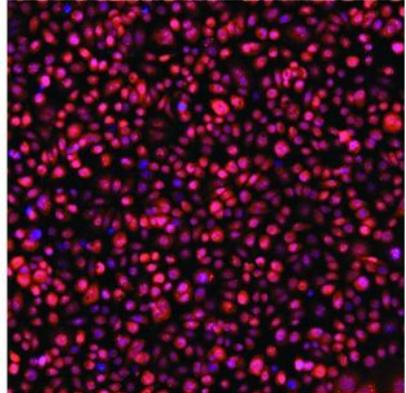
b$_3$. Control cells (AGS)

Figure 5

Impaired protein translation in a1) MCF7 and b1) AGS mediated by MazF. a2, b2: The reduction of fluorescence (red signals) indicated the inhibition of nascent protein synthesis in transfected cells. The nucleases were stained with NuclearMask Blue stain, (n=3).
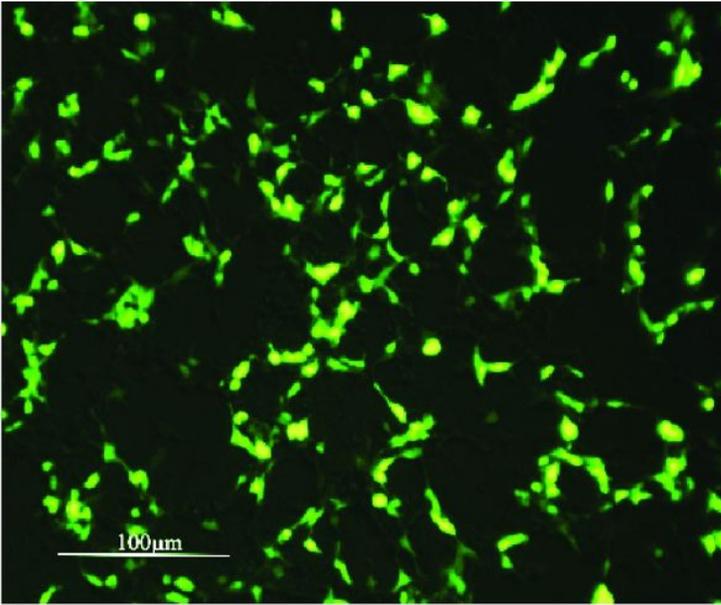
a. HEK293 transfected with pcDNA3.3-egfp
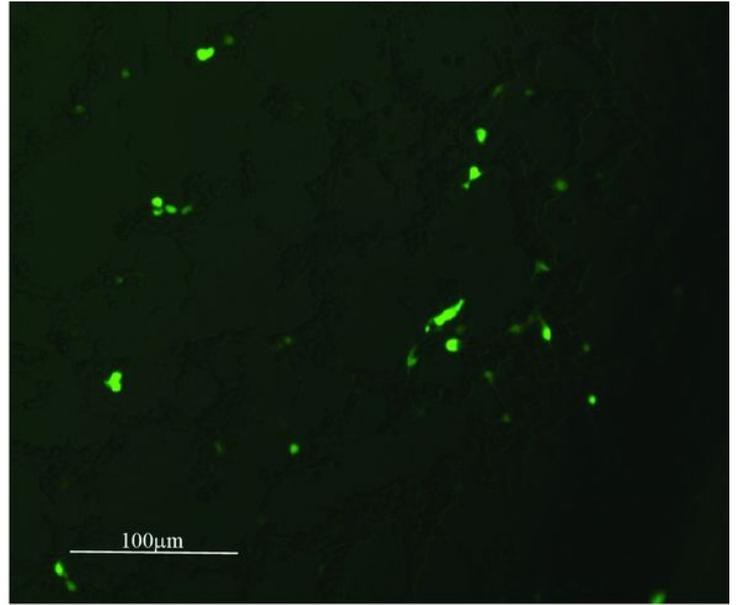
b. HEK293 co-transfected with pcDNA3.3-egfp and C-mazF-A mRNA

Figure 6

Impact on pcDNA3.3-egfp expression in C-mazF-A mRNA transfected HEK 293 cells. a) Abundant GFP expression in HEK293; b) Reduced GFP expression in C-mazF-A mRNA transfected HEK 293 cells.

Supplementary Files

This is a list of supplementary files associated with this preprint. Click to download.

- Figure4WesternBlotRawData.pptx